Journal of Pharmacopuncture

ISSN 2093-6966 [Print], ISSN 2234-6856 [Online]
Journal of Pharmacopuncture 2016;19[1]:059-069
DOI: http://dx.doi.org/10.3831/KPI.2016.19.008

Original article

Ethanol Extract of *Ganoderma lucidum* Augments Cellular Anti-oxidant Defense through Activation of Nrf2/HO-1

Yoo-hwan Lee[1], Jung-hee Kim[1], Choon-ho Song[1], Kyung-jeon Jang[1], Cheol-hong kim[1], Ji- Sook Kang[2], Yung-hyun Choi[2,3], Hyun-Min Yoon[1]*

[1] Departments of Acupuncture and Moxibustion, Dong-Eui University College of Korean Medicine, Busan, Korea
[2] Anti-Aging Research Center, Dong-Eui University, Busan, Korea
[3] Departments of Biochemistry, Dong-Eui University College of Korean Medicine, Busan, Korea

Key Words

anti-oxidant, *Ganoderma lucidum*, heme oxygenase-1, Nrf2, reactive oxygen species

Abstract

Objectives: The mushroom *Ganoderma lucidum* has been widely used as a traditional herbal medicine for many years. Although several studies have focused on the anti-oxidative activity of this mushroom, the molecular mechanisms underlying its activity have not yet been clearly established. The present study investigated the cytoprotective effect of ethanol extract of *Ganoderma lucidum* (EGL) against oxidative stress (hydrogen peroxide, H_2O_2) and elucidated the underlying mechanisms in a C2C12 myoblast cell line.

Methods: Oxidative stress markers were determined by using the comet assay to measure reactive oxygen species (ROS) generation and deoxyribonucleic acid (DNA) damage. Cell viability and Western blotting analyses were employed to evaluate the cellular response to EGL and H_2O_2 in C2C12 cells. Transfection with nuclear factor erythroid 2-related factor 2 (Nrf2)-specific small interfering ribonucleic acid (siRNA) was conducted to understand the relationship between Nrf2 expression and H_2O_2-induced growth inhibition.

Results: The results showed that EGL effectively inhibited H_2O_2-induced growth and the generation of ROS. EGL markedly suppressed H_2O_2-induced comet-like DNA formation and phosphorylation of histone H2AX at serine 139 (p-γH2AX), a widely used marker of DNA damage, suggesting that EGL prevented H_2O_2-induced DNA damage. Furthermore, the EGL treatment effectively induced the expression of Nrf2, as well as heme oxygenase-1 (HO-1), with parallel phosphorylation and nuclear translocation of Nrf2 in the C2C12 myoblasts. However, zinc protoporphyrin IX, a HO-1 inhibitor, significantly abolished the protective effects of EGL against H_2O_2-induced accumulation of ROS and reduced cell growth. Notably, transient transfection with Nrf2-specific siRNA attenuated the cytoprotective effects and HO-1 induction by EGL, indicating that EGL induced the expression of HO-1 in an Nrf2-dependent manner.

Conclusion: Collectively, these results demonstrate that EGL augments the cellular anti-oxidant defense capacity through activation of Nrf2/HO-1, thereby protecting C2C12 myoblasts from H_2O_2-induced oxidative cytotoxicity.

Received: Jan 24, 2016 **Reviewed**: Feb 14, 2016 **Accepted:** Feb 17, 2016

1. Introduction

The decrease in anti-oxidant mechanisms, together with excessive accumulation of reactive oxygen

***Corresponding Author**
Hyun-Min Yoon. Department of Acupuncture & Moxibustion Meridian & Acupoint, College of Oriental Medicine, Dong-Eui University, San 45-1, Yangjung-2-dong, Busanjin-Gu, Busan 614-710, Korea.
Tel: +82-51-850-8935 Fax: +82-51-867-5162
E-mail: 3rdmed@hanmail.net

species (ROS), including superoxide radical anions, hydroxyl radicals, singlet oxygen, and hydrogen peroxide (H_2O_2), are causally linked to various health problems [1, 2]. Within healthy muscle cells, ROS are generated both as by-products of metabolism and as critical effectors of signaling cascades [3]. However, ROS also have genotoxicological effects, causing damage to major cellular components, including proteins, lipids, and nucleic acids [4, 5]. Excessive generation of ROS in skeletal muscles can influence the contractile function of skeletal muscles by causing fatigue and increasing cell oxidative damages, which is implicated in the development of multiple diseases, including muscular dystrophy and sarcopenia [6, 7]. Therefore, increasing the anti-oxidant capacity of skeletal muscles can play a role in preventing disease, improving muscle performance, and enhancing quality of life.

The fruiting body of *Ganoderma lucidum* (*G. lucidum*; Polyporaceae) has been used as a traditional Oriental medicine in tonics for promoting longevity and health for more than 2000 years in China, Korea, Japan and other Asian countries [8, 9]. Accumulating evidence indicates that this mushroom possesses diverse and potentially significant pharmacological effects, including anti-cancer, anti-inflammatory, anti-diabetic, and anti-bacterial effects, in addition to hepatoprotective, neuroprotective, and immunoenhancing activities [8, 10-19]. Studies also suggest that *G. lucidum* possesses strong anti-oxidant properties, which protect cells against oxidative-induced damage through the induction of phase II enzymes, such as heme oxygenase-1 (HO-1), quinone reductase, glutathione S-transferase (GST), and glutathione reductase [20-25]. *G. lucidum* was reported to protect macrophages against inflammatory stress *via* the activation of the nuclear factor erythroid 2-related factor 2 (Nrf2), mediated by the expression of HO-1 [22]. However, to date, the mechanisms underlying the inhibition of oxidative stress by *G. lucidum* have not been well characterized.

Nrf2, a basic leucine zipper transcription factor ubiquitously expressed in most tissues, is a master cellular sensor of oxidative stress and represents the primary response to changes in the cellular redox state [26, 27]. Under normal conditions, Nrf2 is bound to Kelch-like ECH-associated protein 1 (Keap1) in the cytoplasm. Phase II enzyme inducers can disrupt the Nrf2/Keap1 complex, resulting in the release of Nrf2 and its subsequent translocation to the nucleus [28, 29]. In the nucleus, Nrf2 binds with and activates the anti-oxidant response element (ARE), a cis-acting enhancer present in the promoter region of a large and distinct set of target genes, with the aim of restoring redox homeostasis [27, 30]. HO-1 was reported to be active in protecting cells exposed to oxidizing agents by catalyzing the oxidation of heme to biologically active products, including carbon monoxide, biliverdin, and ferrous iron [31]. The final products of heme catabolism exert anti-oxidant effects by neutralizing intracellular ROS [32, 33]. Moreover, enhanced HO-1 expression, which is mainly regulated by the Nrf2-ARE pathway, is associated with protection against stress, such as oxidative stress [26, 34, 35]. Recent studies reported that the stabilization or phosphorylation of the Nrf2 protein increased the activation of the Nrf2/HO-1 pathway. Several signaling molecules have been shown to participate in this process in response to a variety of phase II gene inducers [36, 37]. Therefore, pharmacological activation of Nrf2/HO-1 signaling is critical for the protection of cells exposed to oxidative stress. The present study investigated the ability of an ethanol extract of *G. lucidum* (EGL) to protect cells from H_2O_2-induced cell damage and to elucidate the mechanism underlying those protective effects by using a mouse myoblast C2C12 cell line.

2. Materials and Methods

EGL was supplied by the Department of Acupuncture and Moxibustion, Dongeui University College of Korean Medicine (Busan, Korea). For the preparation of EGL, freeze-dried and milled *G. lucidum* fruiting bodies (200 g) were extracted with 25% ethanol (4 L) at room temperature for 10 hours by using a blender. The extracts were filtered through a Whatman no. 2 filter (pore size: 0.22 μm, Whatman, Maidstone, UK), concentrated to 500 mL under vacuum conditions and then stored at — 20°C [38]. The EGL solution was directly diluted in culture medium to the desired concentration prior to use.

The C2C12 mouse myoblast cell line was obtained from the American Type Culture Collection (Manassas, VA, USA). The cells were grown in Dulbecco's modified Eagle's medium (GibcoBRL, Gaithersburg, MD, USA) and supplemented with 10% heat-inactivated fetal bovine serum (GibcoBRL) and 100 μg/mL of penicillin/streptomycin antibiotics in a humidified 5% CO_2 atmosphere at 37°C. Nrf2 small interfering ribonucleic acid (siRNA) and control siRNA were purchased from Santa Cruz Biotechnology, Inc. Lipofectamine® RNAiMAX transfection reagent (Invitrogen, Carlsbad, CA, USA) was used according to the manufacturer's instructions to transfect the siRNA into the cells. For transfection, the cells were seeded in 6-well culture plates and incubated with the control siRNA or Nrf2 siRNA at 50 nM for 6 hours in serum-free OPTI-MEM media (Invitrogen). After incubation, the transfected cells were subjected to the treatment described in the Fig. 6.

For the cell viability assay, C2C12 cells were seeded in 6-well plates at a density of 1×10^5 cells per well. After incubation for 24 hours, the cells were treated with EGL at different concentrations in the presence or absence of H_2O_2 (Sigma-Aldrich Chemical Co., St. Louis, MO, USA), zinc protoporphyrin IX (ZnPP; Sigma-Aldrich Chemical Co.) or N-acetyl-L-cysteine (NAC, Sigma-Aldrich Chemical Co.). After incubation for 24 hours, the medium was discarded, and the cells were incubated with 0.5 mg/mL of 3-[4,5-dimethylthiazol-2-yl]-2,5-diphenyltetrazolium bromide (MTT, Sigma-Aldrich Chemical Co.) solution for 3 hours at 37°C. The supernatant was discarded, and the formazan blue that formed in the cells was dissolved in dimethyl sulfoxide (DMSO, Sigma-Aldrich Chemical Co.). The optical density was then measured at 540 nm by using an enzyme-linked immunosorbent assay (ELISA) plate reader (Dynatech MR-7000; Dynatech Laboratories, Chantilly, VA, USA).

The measurement of the ROS was performed using ROS-sensitive 2′,7′-dichlorodihydrofluorescein diacetate

(DCF-DA, Molecular Probes, Eugene, OR, USA) reagent, a fluorescent dye that visualizes ROS. Briefly, the cells were incubated with 10-μM DCF-DA for 30 minutes at room temperature in the dark. Spectrofluorimetry analysis using an ELISA plate reader was performed to quantify the intracellular ROS at excitation and emission wavelengths of 488 and 525 nm, respectively.

To assess deoxyribonucleic acid (DNA) damage, we mixed the cell suspension with 0.5% low-melting agarose (LMA) at 37°C, and we spread the mixture on a fully-frosted microscopic slide, which had been pre-coated with 1% normal-melting agarose. After the solidification of the agarose, the slide was covered with 0.5% LMA and was subsequently immersed in a lysis solution [2.5-M sodium chloride (NaCl), 100-mM Na-ethylenediaminetetraacetic acid (EDTA), 10-mM Tris, 1% Triton X100, and 10% DMSO (pH 10)] for 1 hour at 4°C. The slides were placed in a gel electrophoresis apparatus containing 300-mM sodium hydroxide (NaOH) and 10-mM Na-EDTA (pH 13) for 40 minutes to allow for the unwinding of the DNA and for the expression of alkali-labile damage. An electrical field was then applied (300 mA, 25 V) for 20 minutes at 4°C to draw the negatively-charged DNA toward the anode. After electrophoresis, the slides were washed three times for 5 minutes each time at 4°C in a neutralizing buffer (0.4-M Tris, pH 7.5), followed by staining with 20 μg/mL of propidium iodide (Sigma-Aldrich Chemical Co.). The slides were washed twice with phosphate buffer saline (PBS), and images were then captured using a fluorescence microscope (Carl Zeiss, Oberkochen, Germany). The images were also analyzed using an image analysis system (Komet 5.5, Kinetic Imaging, Liverpool, UK) to evaluate the degree of DNA damage. The tail length and moment were used as measures of the extent of the DNA damage. One hundred cells were randomly selected and measured (two slides made for one sample, 50 randomly-selected cells per slide) from one sample. The values of the mean tail length per sample and the percentages of cells with different tail lengths (i.e., undamaged cells without a tail, cells with a tiny tail, cells with a dim tail, cells with a clear tail, and cells with only a tail) were calculated [39].

To prepare the whole-cell proteins, we collected and lysed cells with lysis buffer (25 mM of Tris-Cl (pH 7.5), 250 mM of NaCl, 5 mM of EDTA, 1% Nonidet P-40, 0.1 mM of sodium orthovanadate, 2 μg/mL of leupeptin, and 100 μg/mL of phenylmethylsulfonyl fluoride) containing protease inhibitor cocktail tablets for 30 minutes at 4°C. In a parallel experiment, nuclear and cytosolic proteins were prepared using nuclear extraction reagents (Pierce Biotechnology, Rockford, IL, USA) according to the manufacturer's protocol. The cell debris was discarded following centrifugation at 13,000 g for 15 minutes, and the supernatants were collected. The protein content was determined using a BioRad protein assay reagent (BioRad, Hercules, CA, USA) according to the manufacturer's instructions. For Western blot analyses, equal amounts of protein extracts were subjected to electrophoresis on sodium dodecyl sulfate (SDS)-polyacrylamide gels and subsequently transferred onto nitrocellulose membranes (Schleicher & Schuell Bioscience, Inc., Keene, NH, USA) by electroblotting. The membranes were blocked with 5% skimmed milk for 1 hour at room temperature and incubated overnight with primary antibodies (Cell Signaling Technology, Inc., Boston, MA, USA; Santa Cruz Biotechnology, Santa Cruz, CA, USA; Abcam, Inc., Cambridge, UK), followed by incubation for 1 hour with horseradish peroxidase-conjugated donkey anti-rabbit and sheep anti-mouse immunoglobulin (Amersham Biosciences, Arlington Heights, IL, USA). The immunoreactive bands were revealed by using enhanced chemiluminescence (ECL) with a commercially-available ECL kit (Amersham Biosciences) according to the recommended procedure. Actin and poly [adenosine diphosphate (ADP)-ribose] polymerase (PARP) were used as internal controls for total cellular and nuclear proteins, respectively.

Data from at least three independent experiments were expressed as the mean ± standard deviation (SD). Statistical comparisons between the different groups were performed using a one-way analysis of variance (ANOVA), followed by Student's *t*-tests, after comparing each treated group to the negative control. Values of $P < 0.01$ were considered statistically significant.

3. Results

To evaluate the protective effect of EGL on H_2O_2-induced cytotoxicity, we treated the C2C12 cells with various concentrations of EGL for 24 hours, and the optimal dose (i.e., the dose that had the least effect on cell viability) was selected by determining the percentage of MTT reduction. As shown in Fig. 1A, treatment of the cell cultures with 5 — 50 μg/mL of EGL for 24 hours had no effect on the cell viability. However, 100 μg/mL EGL induced a partial reduction in the cell viability. Thus, 50 μg/mL of EGL was chosen as the highest optimal dose for studying the cytoprotective effect of EGL against H_2O_2-induced cell damage. To determine the protective effects of EGL against H_2O_2-induced cytotoxicity in the C2C12 cells, we pretreated the cells with EGL for 1 hour and exposed them to H_2O_2 for an additional 24 hours. The viability of the C2C12 cells when exposed to H_2O_2 at a concentration of 1 mM for 6 hours decreased significantly as compared with that of the control group, and the survival rate was approximately 58.70% that of the control. However, when the C2C12 cells were pretreated with 25 and 50 μg/mL of EGL, the cell viability significantly increased as compared with that of the H_2O_2 group, and the survival rates were 71.20% and 81.70% that of the control, respectively (Fig. 1B).

To examine the inhibitory effect of EGL on H_2O_2-induced ROS production, we stimulated the C2C12 cells with 1-mM H_2O_2 for 30 minutes in the presence or absence of 50 μg/mL of EGL; then, we determined the intracellular levels of ROS. Compared to the non-treated control cells, the C2C12 cells treated with 1-mM H_2O_2 for 30 minutes showed levels of intracellular ROS that were markedly increased, as indicated by an increase in the DCF-liberated fluorescent signal (Fig. 1C). However, pretreatment with EGL significantly reduced H_2O_2-induced ROS production as compared with that of the control. As a positive control, 10-mM NAC, a specific ROS scavenger, also markedly attenuated H_2O_2-induced generation of ROS. The results indicate that EGL possesses scavenging activity, preventing the accu-

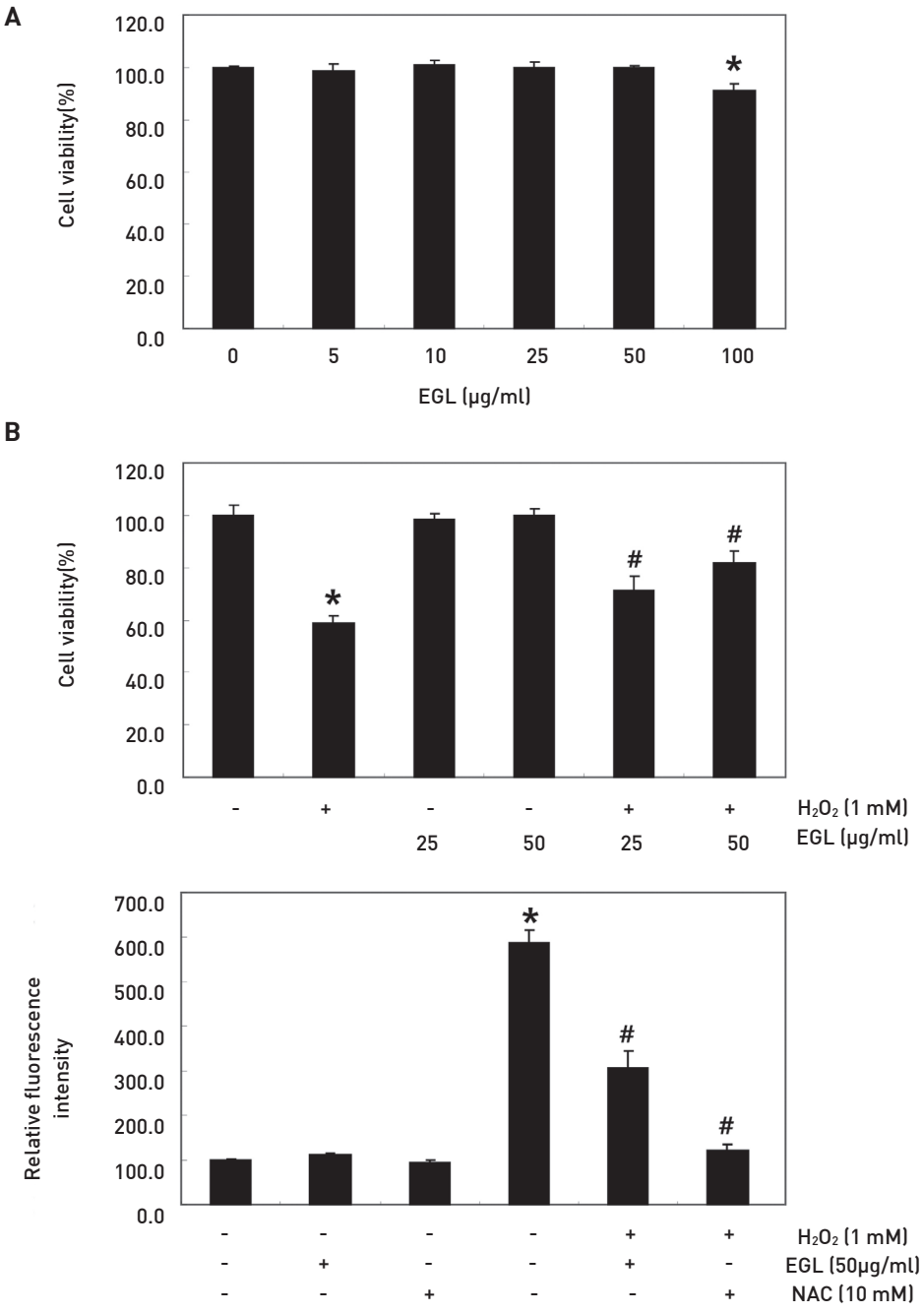

Figure 1 Effects of EGL on the inhibition of H_2O_2-induced cell growth and the generation of ROS in C2C12 myoblasts.

The cells were (A) treated with various concentrations of EGL for 24 hours or (B) pretreated with the indicated concentrations of EGL for 1 hour and then incubated for 24 hours in the presence and absence of 1.0-mM H_2O_2. The cell viability was estimated by using an MTT reduction assay. (C) The cells were pretreated with 50 μg/mL of EGL or 5-mM NAC for 1 hour and then stimulated for 30 minutes with or without 1.0-mM H_2O_2. The cells were incubated at 37°C in the dark for 20 minutes with culture medium containing 10-μM DCF-DA to monitor ROS production. ROS generation was measured by using flow cytometry. The results are the mean ± SD values obtained from three independent experiments ($^{*}P < 0.05$ compared with the untreated control group; $^{\dagger}P < 0.05$ compared with the H_2O_2-treated group). EGL, extract of *Ganoderma lucidum*; H_2O_2, hydrogen peroxide; ROS, reactive oxygen species; MTT, 3-[4,5-dimethylthiazol-2-yl]-2,5-diphenyltetrazolium bromide; NAC, N-acetyl-L-cysteine; DCF-DA, 2′,7′-dichlorodihydrofluorescein diacetate; SD, standard deviation.

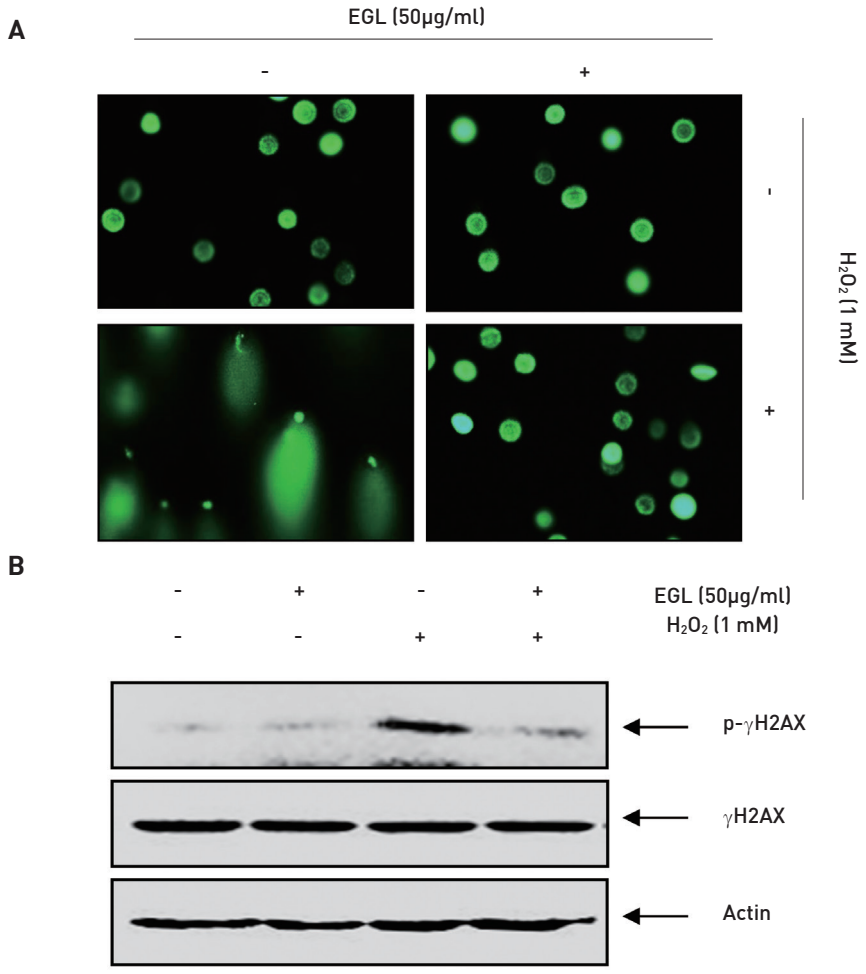

Figure 2 Effects of EGL on H_2O_2-induced DNA damage and γH2AX phosphorylation in C2C12 myoblasts.

(A) The cells were pretreated with EGL for 1 hour and then incubated in the presence or absence of 1.0-mM H_2O_2 for 24 hours. A comet assay was performed to detect cellular DNA damage, and representative photographs of the comets were taken using a fluorescence microscope (200 × original magnification). (B) Cellular proteins and isolated cells grown under the same conditions as (A) were separated on SDS-polyacrylamide gels and transferred to nitrocellulose membranes. The membranes were probed with specific antibodies against p-γH2AX and γH2AX. Actin was used as an internal control.
EGL, extract of *Ganoderma lucidum*; H_2O_2, hydrogen peroxide; DNA, deoxyribonucleic acid; p-γH2AX, phosphorylation of histone H2AX at serine 139; SDS, sodium dodecyl sulfate.

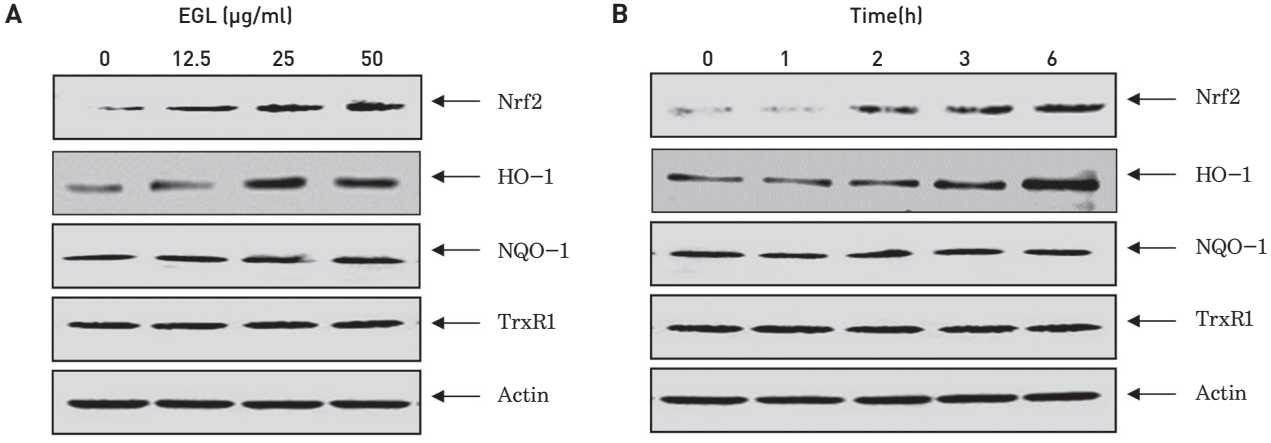

Figure 3 Effects of EGL on the levels of Nrf2, HO-1, NQO-1, and TrxR1 in C2C12 myoblasts.

(Continued)

The cells were incubated either (A) with various concentrations of EGL for 6 hours or (B) with 50 μg/mL of EGL for the indicated periods. Cellular proteins were separated on SDS-polyacrylamide gels and transferred to nitrocellulose membranes. The membranes were probed with specific antibodies against Nrf2, HO-1, and TrxR1. Actin was used as the loading control.
EGL, extract of *Ganoderma lucidum*; Nrf2, nuclear factor erythroid 2-related factor 2; HO-1, heme oxygenase-1; NQO-1, nicotinamide quinone oxidoreductase 1; TrxR1, thioredoxin reductase 1; SDS, sodium dodecyl sulfate.

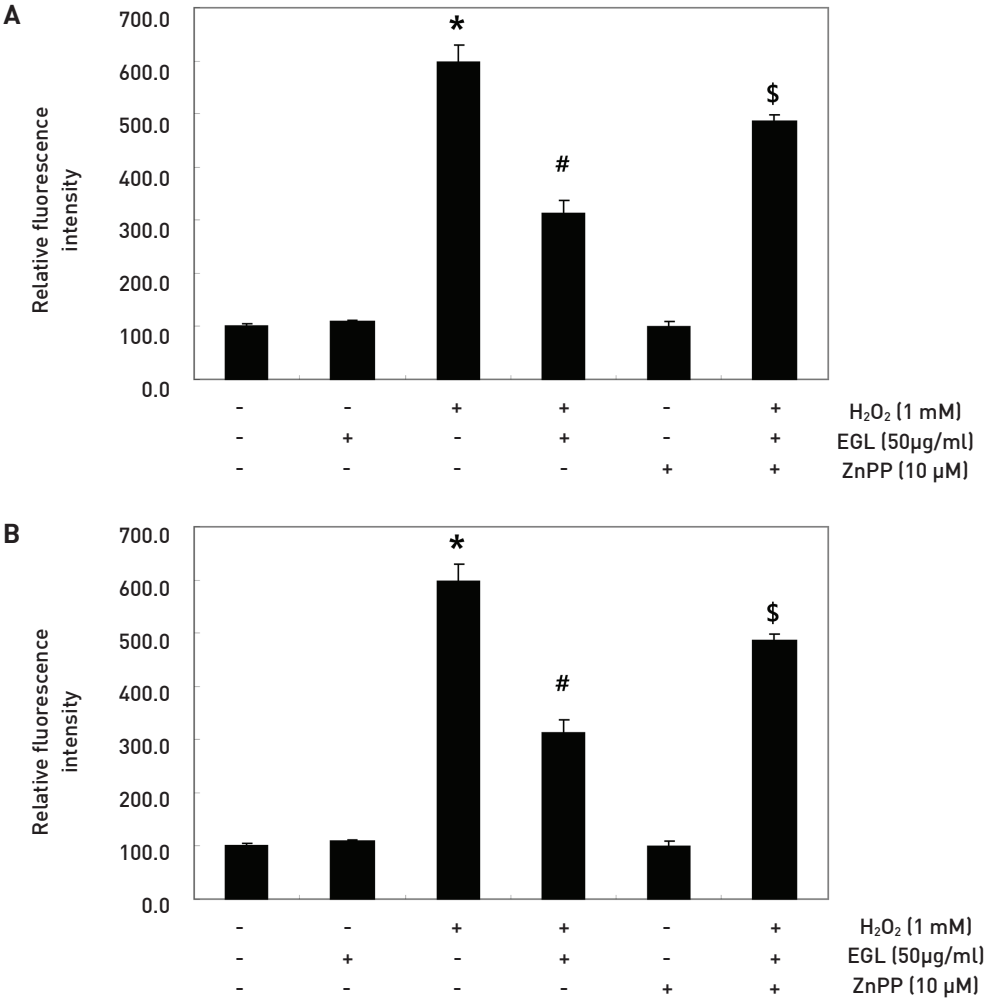

Figure 4 EOD enhanced ROS accumulation in HT-29 cells.

The cells were pretreated for 1 hour with 50 μg/mL of EGL and then treated for (A) 30 minutes or (B) 24 hours with or without 1.0-mM H_2O_2 in the absence or presence of 10-μM ZnPP. (A) After incubation with 10-μM JC-1 for 20 minutes, JC-1 fluorescence intensity was detected using a flow cytometer. (B) The cell viability was assessed using an MTT reduction assay. The results are the mean ± SD values obtained from three independent experiments ($^{*}P < 0.05$ compared with the untreated group; $^{\dagger}P < 0.05$ compared with the H_2O_2-treated group; $^{\ddagger}P < 0.05$ compared with the H_2O_2- and EGL-treated groups).
HO-1, heme oxygenase-1; EGL, extract of *Ganoderma lucidum*; H_2O_2, hydrogen peroxide; ROS, reactive oxygen species; Znpp, zinc protoporphyrin IX; JC-1, 5,5′,6,6′-tetrachloro-1,1′,3,3′-tetraethylbenzimidazolylcarbocyanine Iodide; MTT, 3-[4,5-dimethylthiazol-2-yl]-2,5-diphenyltetrazolium bromide; SD, standard deviation.

mulation of ROS generated by H_2O_2 in C2C12 myoblasts.

Oxidative stress-induced DNA damage produces lesions that lead to a loss of cell viability. H_2O_2-mediated DNA damage in the C2C12 cells was detected using an alkaline comet assay (single-cell gel electrophoresis) and a Western blot analysis. The comet assay revealed that the treatment with H_2O_2 alone significantly increased the number of DNA breaks, enhancing the fluorescence intensity in the tails of the comet-like structures associated with an increase in the tail length and moment (Fig. 2A, Table 1). In contrast, the untreated control cells showed only typical, representative nuclei. The pretreatment with EGL markedly prevented the adverse effects. An immunoblot image revealed that the levels of phosphorylation of nuclear histone H2AX (p-γH2AX) at serine 139, a sensitive marker of DNA double-strand break formation [40], were markedly

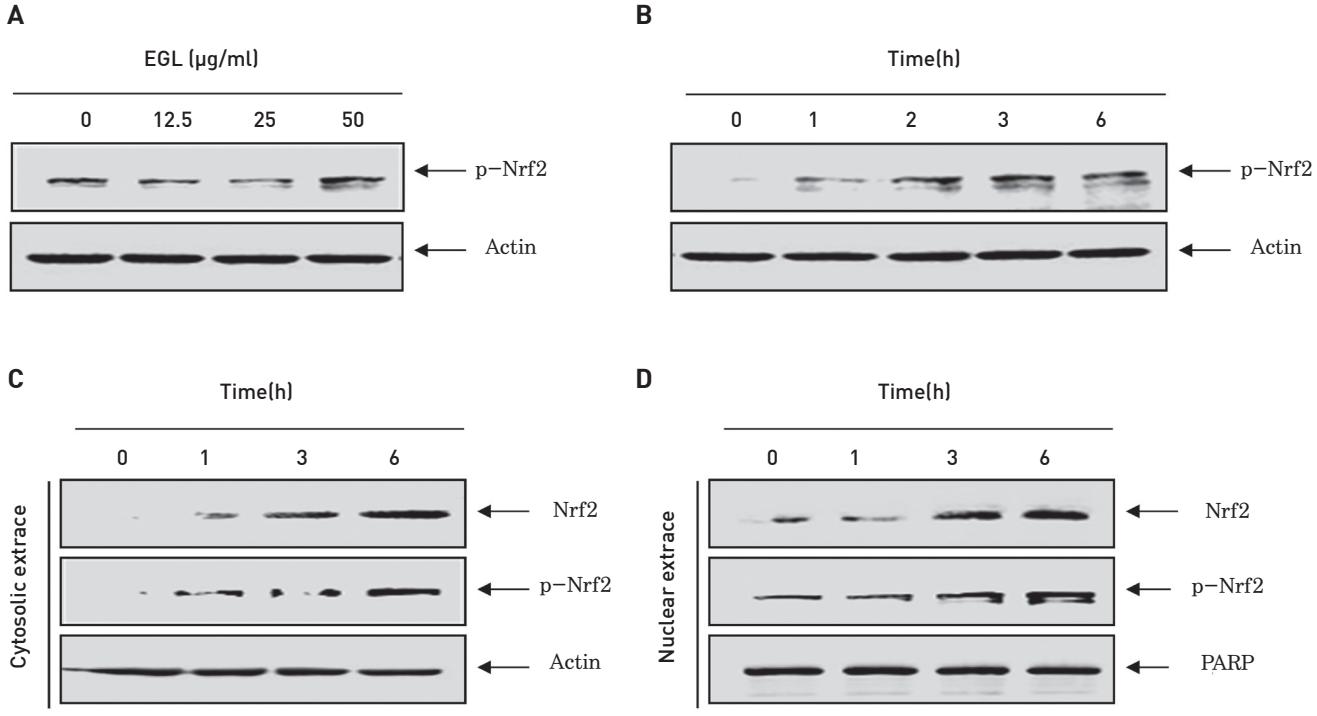

Figure 5 EGL-induced phosphorylation and nuclear translocation of Nrf2 in C2C12 myoblasts.

The cells were incubated (A) with various concentrations of EGL for 6 hours or (B-D) with 50 μg/mL of EGL for the indicated periods. Total (A and B), cytosolic (C), or nuclear (C) proteins were separated on SDS-polyacrylamide gels and then transferred onto nitrocellulose membranes. The membranes were probed with anti-Nrf2 and anti-p-Nrf2 antibodies. Proteins were visualized using an ECL detection system. Actin and PARP were used as the internal controls of cytosolic and nuclear proteins, respectively.
EGL, extract of *Ganoderma lucidum*; Nrf2, nuclear factor erythroid 2-related factor 2; SDS, sodium dodecyl sulfate; ECL, enhanced chemiluminescence; PARP, polymerase.

increased in the H_2O_2-treated C2C12 cells (Fig. 2B). In contrast, the expression of p-γH2AX decreased significantly in the EGL-pretreated cells, indicating that EGL helped to protect against DNA damage induced by oxidative stress.

As regulation by Nrf2 signaling of the cellular anti-oxidant response has been well documented [27, 30], we next examined whether EGL protected cells from oxidative stress by activating the Nrf2 signaling pathway. The immunoblotting results indicated that the EGL treatment effectively induced the expression of the Nrf2 protein in a concentration- and time-dependent manner in the C2C12 cells (Fig. 3). The results also showed that the EGL treatment induced the expression of the HO-1 protein, an Nrf2 target gene, in the C2C12 cells (Fig. 3). However, the EGL treatment had no effect on other anti-oxidant enzymes, such as nicotinamide adenine dinucleotide phosphate (NADPH)-quinone oxidoreductase 1 (NQO-1) and thioredoxin reductase 1 (TrxR1) (Fig. 3).

To investigate the role of HO-1 induction in EGL-mediated protective effects against oxidative stress in the C2C12 cells, we applied ZnPP, a selective inhibitor of HO-1, in the present study. As indicated in Fig. 4A, ZnPP significantly reversed the inhibition of ROS generation by EGL in the H_2O_2-stimulated C2C12 cells. In addition, the results of the MTT assay showed that the addition of ZnPP significantly attenuated the protective effect of EGL against H_2O_2-induced cytotoxicity (Fig. 4B), suggesting that the cytoprotective effect of EGL was partly mediated by HO-1 induction.

As the phosphorylation of Nrf2 at Ser40 by several kinases is a critical process in its stabilization and nuclear translocation [30, 36, 37], the phosphorylation of Nrf2 in the EGL-treated cells was examined to confirm whether Nrf2 was induced by EGL. As shown in Figs. 5A and 5B, the EGL treatment caused concentration- and time-dependent increases in the levels of phosphorylated Nrf2 expression. Additionally, a Western blot analysis was carried out using the nuclear and the cytosolic fractions of the C2C12 cells to determine whether EGL promoted the nuclear translocation of Nrf2. As shown in Figs. 5C and 5D, the amounts of total and phosphorylated Nrf2 proteins in the nucleus were markedly increased following exposure to EGL, indicating that EGL induced the translocation of Nrf2 from the cytosol to the nucleus.

We next developed an Nrf2 gene knockdown model by using siRNA transfection to demonstrate the contribution of Nrf2 signaling to the negative effects of EGL on H_2O_2-induced cytotoxicity. The results of a Western blot analysis indicated that the silencing of Nrf2 by using specific siRNA greatly reduced the EGL-induced expression of Nrf2 compared with that of the untransfected control cells and the control siRNA-transfected cells (Fig. 6A). Therefore,

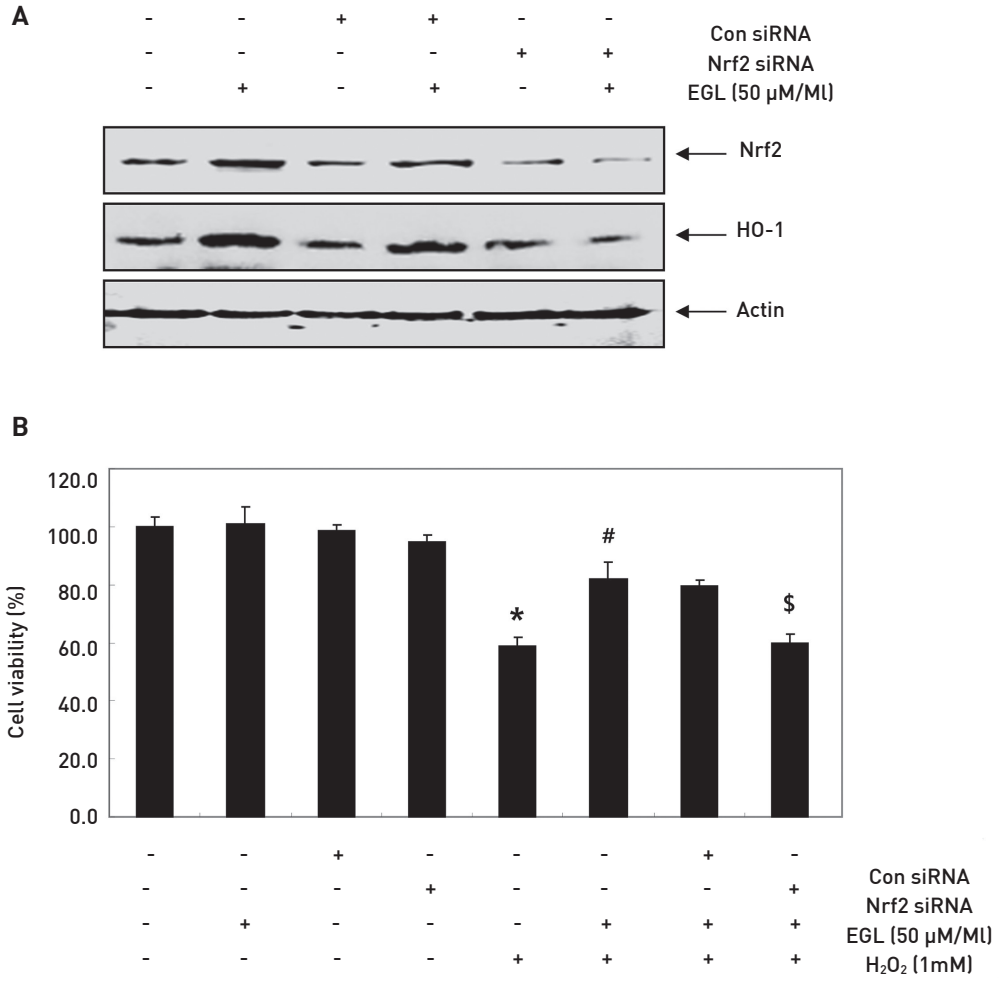

Figure 6 Nrf2-dependent induction of HO-1 by EGL in C2C12 myoblasts.

(A) The cells were transfected with control (Con siRNA, as a negative control for the RNA interference) and Nrf2 siRNA. After 24 hours, the cells were treated for 6 hours with or without 50 μg/mL of EGL. The proteins were separated on SDS-polyacrylamide gels and then transferred onto nitrocellulose membranes. The membranes were probed with the specific antibodies against Nrf2 and HO-1. Proteins were visualized using an ECL detection system. Actin was used as an internal control. (B) The cells were transfected with control and Nrf2 siRNA. After 24 hours, the cells were treated with 50 μg/mL of EGL for 24 hours or pretreated with 50 μg/mL of EGL for 1 hour. They were then incubated in the presence or absence of 1.0-mM H_2O_2 for 24 hours. The cell viability was estimated using an MTT reduction assay. The results are the mean ± SD values obtained from three independent experiments ($^*P < 0.05$ compared with the untreated group; $^\dagger P < 0.05$ compared with the H_2O_2-treated group; $^\ddagger P < 0.05$ compared with the H_2O_2- and EGL-treated groups).
Nrf2, nuclear factor erythroid 2-related factor 2; HO-1, heme oxygenase-1; EGL, extract of *Ganoderma lucidum*; siRNA. small interfering ribonucleic acid; SDS, sodium dodecyl sulfate; ECL, enhanced chemiluminescence; H_2O_2, hydrogen peroxide; MTT, 3-[4,5-dimethylthiazol-2-yl]-2,5-diphenyltetrazolium bromide; SD, standard deviation.

Table 1 Preventive effect of EGL on H_2O_2-induced DNA damage in C2C12 cells (mean ± SD)

Compounds	Scored cells	Tail moment	Tail length
Control	100	2.69 ± 0.97	59.10 ± 3.49
EGL (50 μg/mL)	100	2.15 ± 1.45	61.56 ± 10.81
H_2O_2 (1.0 mM)	100	52.09 ± 3.96	169.55 ± 8.91
EGL + H_2O_2	100	6.45 ± 1.09	84.76 ± 5.12

EGL, extract of *Ganoderma lucidum*; H_2O_2, hydrogen peroxide; DNA, deoxyribonucleic acid; SD, standard deviation.

we investigated whether Nrf2 siRNA transfection blocked EGL-induced up-regulation of HO-1 and found that Nrf2 siRNA attenuated these effects, providing evidence that Nrf2 mediated EGL-induced augmentation of HO-1. Furthermore, Nrf2 siRNA significantly cancelled the protective effect of EGL against the H_2O_2-induced reduction of cell viability (Fig. 6B).

4. Discussion

Although few studies have investigated how oxidative stress quantitatively affects the load-carrying capacity of muscle cells [6, 7], oxidative stress is known to accompany muscle dysfunction [3, 7]. Oxidative stress occurs when the production of ROS exceeds their catabolism. ROS belong to a class of endogenous signaling molecules, the functions of which depend on their subcellular localization, local concentration, and duration of production. Moderate levels of ROS transiently oxidize cysteine sulphydryl, which contributes to the active sites of most proteins [4, 5]. However, when the accumulation of ROS exceeds a certain threshold, ROS have adverse effects on cellular functions [1, 4], leading to cellular dysfunction and cell death in skeletal muscles [6, 7]. The mitochondrial electron transport system is a major source of intracellular ROS generation [3-5], with mitochondria playing a pivotal role in the ROS-mediated cell-death process. H_2O_2 directly induces mitochondrial dysfunction, followed by a rapid efflux of intracellular ROS, which increases the permeabilization and depolarization of the mitochondrial membrane [1, 4]. Therefore, the discovery of a reagent that could reduce the levels of ROS would be valuable in the treatment of muscle-related diseases.

This study, which is part of a research program to derive new anti-oxidant agents from medicinal mushrooms, used a C2C12 myoblast cell model to discover whether EGL conferred protection against oxidative stress-induced cytotoxicity. The results indicated that H_2O_2 treatment of C2C12 cells caused marked intracellular accumulations of ROS and inhibited cell survival. However, pretreatment of the C2C12 cells with EGL significantly attenuated the H_2O_2-induced generation of ROS and inhibition of cell viability. Thus, we conjectured that EGL might improve the mitochondrial function by eliminating the H_2O_2-induced overproduction of ROS. In addition, the present study showed that H_2O_2 treatment increased the DNA tail moment and length on a comet assay and the expression of p-γH2AX, both of which are widely-used markers for the detection of DNA damage [40]. The EGL treatment markedly reduced these increases, indicating that EGL provided protection against H_2O_2-induced apoptosis by reducing DNA damage caused by oxidative stress in C2C12 myoblasts.

Recent studies have suggested that Nrf2 plays an indispensable role in protecting a variety of tissues from a wide array of toxic insults, including oxidative stress [27, 29]. Although the role of Nrf2 signaling has not been previously characterized in skeletal muscles, coordinated regulation of Nrf2 redox signaling is believed to preserve the redox state and protect the structure and the function of skeletal muscles [2, 27]. Previous studies demonstrated increased Nrf2 levels in active skeletal muscles and subsequent activation of its major target anti-oxidant enzymes, including HO-1 [1, 2]. They also showed that the loss of Nrf2 was strongly coupled with dysregulation of anti-oxidant pathways and progression of muscle dysfunction [2, 3, 6]. Therefore, Nrf2/HO-1 signaling may represent a potential therapeutic target in the management of oxidative stress-related diseases. Studies have proposed that the induction of phosphorylation plays a key role in the regulation of the transcriptional activity of Nrf2 [36, 37]. A number of protein kinases have been implicated in the regulation of Nrf2 activity, with upstream signals facilitating the translocation of Nrf2 into the nucleus, whereupon it binds to ARE in promoter regions [2-30]. In the present study, we found that EGL increased the expression of the Nrf2 protein in C2C12 myoblasts in a concentration- and duration-dependent manner. Subsequently, we found that EGL triggered the induction of HO-1 expression and led to Nrf2 phosphorylation, along with concomitant translocation of Nrf2 into the nuclei. However, ZnPP-induced inhibition of the expression of HO-1 significantly weakened the inhibitory effects of EGL on H_2O_2-induced inhibition of cell growth by blocking the generation of ROS. In addition, the knockdown of Nrf2 by Nrf2-targeted siRNA completely abrogated EGL-induced HO-1 expression. This finding suggests that Nrf2 is a critical upstream regulator of EGL-mediated induction of HO-1 in C2C12 myoblasts. Furthermore, the knockdown of Nrf2 halted the ability of EGL to restore the growth of C2C12 cells inhibited by H_2O_2. These results suggest that the Nrf2-dependent induction of HO-1 by EGL may participate, at least partly, in the protection against oxidative stress in C2C12 myoblasts.

5. Conclusion

In summary, the results of this study clearly demonstrate that EGL provided protection against H_2O_2-induced cytotoxicity and DNA damage in C2C12 myoblasts through suppression of intracellular ROS generation. Overall, the results imply that EGL may activate Nrf2 signaling and contribute to the induction of the phase II anti-oxidant HO-1 in C2C12 cells, thereby contributing, at least partly, to a cellular defense mechanism against oxidative stress-induced genotoxic events. These findings suggest that EGL may be a potential anti-oxidant agent in C2C12 myoblasts.

Acknowledgment

This research was supported by the Basic Science Research Program through a National Research Foundation of Korea (NRF) grant funded by the Korea government (2015R1A2A2A01004633).

Conflict of interest

The authors declare that there are no conflict of interest.

ORCID

Hyun-Min Yoon. http://orcid.org/0000-0003-3645-6109.

References

1. Szczesny B, Olah G, Walker DK, Volpi E, Rasmussen BB, Szabo C, *et al*. Deficiency in repair of the mitochondrial genome sensitizes proliferating myoblasts to oxidative damage. PLoS One. 2013;8(9):e75201.
2. Miller CJ, Gounder SS, Kannan S, Goutam K, Muthusamy VR, Firpo MA, *et al*. Disruption of Nrf2/ARE signaling impairs antioxidant mechanisms and promotes cell degradation pathways in aged skeletal muscle. Biochim Biophys Acta. 2012;1822(6):1038-50.
3. Ji LL, Gomez-Cabrera MC, Vina J. Exercise and hormesis: activation of cellular antioxidant signaling pathway. Ann N Y Acad Sci. 2006;1067:425-35.
4. Forman HJ. Use and abuse of exogenous H_2O_2 in studies of signal transduction. Free Radic Biol Med. 2007;42(7):926-32.
5. Halliwell B. Oxidative stress and neurodegeneration: where are we now?. J Neurochem. 2006;97(6):1634-58.
6. Song W, Kwak HB, Lawler JM. Exercise training attenuates age-induced changes in apoptotic signaling in rat skeletal muscle. Antioxid Redox Signal. 2006;8(3-4):517-28.
7. Powers SK, Jackson MJ. Exercise-induced oxidative stress: cellular mechanisms and impact on muscle force production. Physiol Rev. 2008;88(4):1243-76.
8. Sanodiya BS, Thakur GS, Baghel RK, Prasad GB, Bisen PS. *Ganoderma lucidum*: a potent pharmacological macrofungus. Curr Pharm Biotechnol. 2009;10(8):717-42.
9. Wachtel-Galor S, Tomlinson B, Benzie IF. *Ganoderma lucidum* ("Lingzhi"), a Chinese medicinal mushroom: biomarker responses in a controlled human supplementation study. Br J Nutr. 2004;91(2):263-9.
10. Cheng S, Sliva D. *Ganoderma lucidum* for cancer treatment: we are close but still not there. Integr Cancer Ther. 2015;14(3):249-57.
11. Yuen JW, Gohel MD, Ng CF. The differential immunological activities of *Ganoderma lucidum* on human pre-cancerous uroepithelial cells. J Ethnopharmacol. 2011;135(3):711-8.
12. Bhardwaj N, Katyal P, Sharma AK. Suppression of inflammatory and allergic responses by pharmacologically potent fungus *Ganoderma lucidum*. Recent Pat Inflamm Allergy Drug Discov. 2014;8(2):104-17.
13. Ma HT, Hsieh JF, Chen ST. Anti-diabetic effects of *Ganoderma lucidum*. Phytochemistry. 2015;114:109-13.
14. Ha do T, Oh J, Khoi NM, Dao TT, Dung le V, Do TN, *et al*. *In vitro* and *in vivo* hepatoprotective effect of ganodermanontriol against t-BHP-induced oxidative stress. J Ethnopharmacol. 2013;150(3):875-85.
15. Lin ZB, Zhang HN. Anti-tumor and immunoregulatory activities of *Ganoderma lucidum* and its possible mechanisms. Acta Pharmacol Sin. 2004;25(11):1387-95.
16. Yoon HM, Jang KJ, Han MS, Jeong JW, Kim GY, Lee JH, *et al*. *Ganoderma lucidum* ethanol extract inhibits the inflammatory response by suppressing the NF-κB and toll-like receptor pathways in lipopolysaccharide-stimulated BV2 microglial cells. Exp Ther Med. 2013;5(3):957-63.
17. Jang KJ, Son IS, Shin DY, Yoon HM, Choi YH. Anti-invasive activity of ethanol extracts of *Ganoderma lucidum* through tightening of tight junctions and inhibition of matrix metalloproteinase activities in human gastric carcinoma cells. J Acupunct Meridian Stud. 2011;4(4):225-35.
18. Lai CS, Yu MS, Yuen WH, So KF, Zee SY, Chang RC. Antagonizing beta-amyloid peptide neurotoxicity of the anti-aging fungus *Ganoderma lucidum*. Brain Res. 2008;1190:215-24.
19. Chen LW, Wang YQ, Wei LC, Shi M, Chan YS. Chinese herbs and herbal extracts for neuroprotection of dopaminergic neurons and potential therapeutic treatment of Parkinson's disease. CNS Neurol Disord Drug Targets. 2007;6(4):273-81.
20. Li B, Lee DS, Kang Y, Yao NQ, An RB, Kim YC. Protective effect of ganodermanondiol isolated from the Lingzhi mushroom against tert-butyl hydroperoxide-induced hepatotoxicity through Nrf2-mediated antioxidant enzymes. Food Chem Toxicol. 2013;53:317-24.
21. Ha TB, Gerhäuser C, Zhang WD, Ho-Chong-Line N, Fourasté I. New lanostanoids from *Ganoderma lucidum* that induce NAD(P)H:quinone oxidoreductase in cultured hepalcic7 murine hepatoma cells. Planta Med. 2000;66(7):681-4.
22. Choi S, Nguyen VT, Tae N, Lee S, Ryoo S, Min BS, *et al*. Anti-inflammatory and heme oxygenase-1 inducing activities of lanostane triterpenes isolated from mushroom *Ganoderma lucidum* in RAW264.7 cells. Toxicol Appl Pharmacol. 2014;280(3):434-42.
23. Hsieh TC, Wu JM. Suppression of proliferation and oxidative stress by extracts of *Ganoderma lucidum* in the ovarian cancer cell line OVCAR-3. Int J Mol Med. 2011;28(6):1065-9.
24. Oluba OM, Adebisi KE, Eidangbe GO, Odutuga AA, Onyeneke EC. Modulatory effect of crude aqueous extract of *Lingzhi* or *Reishi* medicinal mushroom, *Ganoderma lucidum* (higher Basidiomycetes), on hematological and antioxidant indices in plasmodium berghei-infected mice. Int J Med Mushrooms. 2014;16(5):499-506.
25. Li C, Shi L, Chen D, Ren A, Gao T, Zhao M. Functional analysis of the role of glutathione peroxidase (GPx) in the ROS signaling pathway, hyphal branching and the regulation of ganoderic acid biosynthesis in *Ganoderma lucidum*. Fungal Genet Biol. 2015;82:168-80.
26. Sakata Y, Zhuang H, Kwansa H, Koehler RC, Dore S. Resveratrol protects against experimental stroke: putative neuroprotective role of heme oxygenase 1. Exp Neurol. 2010;224(1):325-9.
27. Kobayashi M. Yamamoto M. Molecular mechanisms activating the Nrf2-Keap1 pathway of antioxidant gene regulation. Antioxid Redox Signal. 2005;7(3-4):385-94.
28. Zhang Y, Gordon GB. A strategy for cancer prevention: stimulation of the Nrf2-ARE signaling pathway. Mol Cancer Ther. 2004;3(7):885-93.

29. Niture SK, Khatri R, Jaiswal AK. Regulation of Nrf2-an update. Free Radic Biol Med. 2014;66:36-44.
30. Ishii T, Itoh K, Takahashi S, Sato H, Yanagawa T, Katoh Y, *et al*. Transcription factor Nrf2 coordinately regulates a group of oxidative stress-inducible genes in macrophages. J Biol Chem. 2000;275(21):16023-9.
31. Scapagnini G, Butterfield DA, Colombrita C, Sultana R, Pascale A, Calabrese V. Ethyl ferulate, a lipophilic polyphenol, induces HO-1 and protects rat neurons against oxidative stress. Antioxid Redox Signal. 2004;6(5):811-8.
32. Katori M, Anselmo DM, Busuttil RW, Kupiec-Weglinski JW. A novel strategy against ischemia and reperfusion injury: cytoprotection with heme oxygenase system. Transpl Immunol. 2002;9(2-4):227-33.
33. Motterlini R, Foresti R. Heme oxygenase-1 as a target for drug discovery. Antioxid Redox Signal. 2014;20(11):1810-26.
34. Chapple SJ, Siow RC, Mann GE. Crosstalk between Nrf2 and the proteasome: therapeutic potential of Nrf2 inducers in vascular disease and aging. Int J Biochem Cell Biol. 2012;44(8):1315-20.
35. Jeong WS, Jun M, Kong AN. Nrf2: A potential molecular target for cancer chemoprevention by natural compounds. Antioxid Redox Signal. 2006;8(1-2):99-106.
36. Pi J, Bai Y, Reece JM, Williams J, Liu D, Freeman ML, *et al*. Molecular mechanism of human Nrf2 activation and degradation: role of sequential phosphorylation by protein kinase CK2. Free Radic Biol Med. 2007;42(12):1797-806.
37. Apopa PL, He X, Ma Q. Phosphorylation of Nrf2 in the transcription activation domain by casein kinase 2 (CK2) is critical for the nuclear translocation and transcription activation function of Nrf2 in IMR-32 neuroblastoma cells. J Biochem Mol Toxicol. 2008;22(1):63-76.
38. Jang KJ, Han MH, Lee BH, Kim BW, Kim CH, Yoon HM, *et al*. Induction of apoptosis by ethanol extracts of *Ganoderma lucidum* in human gastric carcinoma cells. J Acupunct Meridian Stud. 2010;3(1):24-31.
39. Osman AG, Mekkawy IA, Verreth J, Wuertz S, Kloas W, Kirschbaum F. Monitoring of DNA breakage in embryonic stages of the African catfish Clarias gariepinus (Burchell, 1822) after exposure to lead nitrate using alkaline comet assay. Environ Toxicol. 2008;23(6):679-87.
40. Rogakou EP, Pilch DR, Orr AH, Ivanova VS, Bonner WM. DNA double-stranded breaks induce histone H2AX phosphorylation on serine 139. J Biol Chem. 1998;273(10):5858-68.